Advances in Concrete Construction, *Vol. 6, No. 5 (2018) 509-525*
DOI: https://doi.org/10.12989/acc.2018.6.5.509

Experimental evaluation of splicing of longitudinal bars with forging welding in flexural reinforced concrete beams

Mohammad K. Sharbatdar*, Omid Mohammadi Jafari[a] and Mohammad S. Karimi[b]

Civil Engineering Faculty, Semnan University, Semnan, Iran

(Received July 13, 2017, Revised December 13, 2017, Accepted September 29, 2018)

Abstract. In this paper the application of forging process as benefit technique in Reinforced Concrete (RC) beam bars and comparison to lap splices was experimentally investigated with four concrete beam specimens with same dimensions and reinforcement details. The reference specimen was with no splices and the other three beams were with different splices (100% forging in the middle, 50% forging, and 100% lap splices in the middle). Beams were tested with the four points load system. Experimental test results indicated that using forging process as new bar splicing method can have high effects on increasing ductility and energy dissipation of concrete structures. It also proved that this method increased the flexural rigidity, energy absorption, and ductility of the RC beams. And also this research results showed that the flexural capacity and ductility of the beam with 50% forging were respectively increased up to 10% and 75% comparing to that of reference specimen, but the energy absorption of this beams was decreased up to 27%. The ductility of beam with 50% forging was increased up to 25% comparing the ductility of beam with 100% forging.

Keywords: forging welding; GPW; flexural capacity; ductility; energy absorption; lap splice

1. Introduction

Discussion about cutting and splicing rebars is one of the important topics raised in the reinforced concrete (RC) structures. There are some methods for splicing rebars such as; rebar overlapping (as the ordinary method), mechanical patching, use of coupler devices, and head to head welding of the rebars (Tahouni 1996). In splicing by overlapping, the length of the rebars to overlap should be at least equal to the anchorage length of the rebars. Due to more length used in overlapped rebars, as a rule of thumb, for the rebars with 30 mm diameter and greater is not cost-efficient. In this circumstances, as an alternate method, use of couplers is proposed which cause the service loads to be decreased, too. Furthermore, use of couplers is a quick and easy installation method, with no need for special tools and skills. Also, in some cases in which the rebars should be patched in situ –e.g., retrofitting of building, or building development, thread-lock couplers may be used. In splicing by thread-lock couplers, end of each rebar -which are going to be

*Corresponding author, Associate Professor, E-mail: msharbatdar@semnan.ac.ir
[a]M.Sc.
[b]Assistant Professor

http://www.techno-press.org/?journal=acc&subpage=7 ISSN: 2287-5301 (Print), 2287-531X (Online)

patched- are placed into the coupler case, next to each other (side by side), and then a wedge-shape nail (looks like a rivet) is pushed in, firmly, between the two rebars to lock them (Bagheri and Fasihi 2013). In mechanical patching, initially, the end of each bar (which are going to be patched) are compressed by special apparatus, to make their diameters about 2 mm bigger than the nominal diameter of the rebar. Then, those two ends are threaded. Bearing patches, as the other kind, are only allowed in rebars under the ever-compressive stresses. Regarding the point that price of reinforcing is of the highest costs, therefore, using less-cost methods to patch rebars can play important role in reducing cost of construction. Welding splice are performed in different types such as; head to head, edge to edge, use of auxiliary parts, and forging which is a modern kind of welding splicing. In this method, two ends of the rebars which are going to be forged, are cut in zero degree by special cutter, quite smoothly and polished. Then, they are merged together under high hydraulic pressure and heat from burning Acetylene gas. The technology of forge welding of the rebars is more cost efficient than conventional methods such as; overlapping, mechanical patching, and coupling. In forging, the strength of the patched region is more than the base material. It has reduction in the project duration and weight of structure; making S shape for a connection and installing by wire take more time than fastening threaded rebars. According to the Uniform Building Code (1997)-B1921-2-6, rebars that are located in moment resistance frame, or in boundary members of the shear walls -which are influenced by the tensile forces and bending moments, due to the earthquake- can be spliced by the mechanical patching, comply with B1921-14-3-4 clause. In the American Concrete Institute regulation (2014) (ACI 318-14), there are limitations to use lap splice for group of rebars, or rebars with diameter greater than 36 mm, and limitation in the panel zone (area of beam-column connection),. Also, splicing in the ever-tensile parts are allowed just only by the mechanical devices and/or welding. According to this code, use of mechanical patches is allowed in all classes of the moment resistance frames, complying with seismic regulations of the mechanical splice. There are similar regulations in the 9th-Iranian National Building code (2013); in which forge welding and also electro-fusion welding are allowed for welding splices.

Some researches had been conducted to assess the effects of type of splicing of the longitudinal bars in flexural beams, by Turk and Yildirim (2003). Navaratnarajah (1983) introduced a new method for splicing of bars by putting two heads of the bars in a steel case and then epoxy adhesive (instead of grout) is injected through it. Some experiments were conducted by McCabe (2000) in the beams under pure bending, in order to assess the favorite performance of the mechanical splices. Some beam-column joints were tested by Reetz *et al*. (2013), so that under cyclic loading the plastic hinge was formed in the effective length of the beam from the column face. This experiments showed that there were some differences in the curvature and other ductility parameters of the joints with and without mechanical splices in the beams. Furthermore, a new method of coupling was assessed by Coogler (2006), in which two ends of rebars (which were going to be patched) were put side by side in special case and then the rivet-like edge-shape nail was pushed in, firmly, between two bars by special devices which make the two rebars locked. El-Hacha *et al*. (2004) assessed the bonding strength and the necessary anchorage length of the bars, spliced by overlapping. Camille *et al*. (2006) studied on side-by-side welding patches in order to get the proper welding length. They suggested the welding length equal to 1.5 times of the bar diameter. Park *et al*. (2008) suggested a kind of nondestructive test to assess the bars spliced by welding method. In this test spliced rebars were put under electro-magnetic current with specific frequency. From the shape of the obtained wave charts, the welding quality was checked. Hua *et al*. (2014) studied on the injection-splice in which the samples were tested under tension.

From the results, the splice length was suggested according to the nominal diameter of bars. Henin and Morcous (2014) tested some injection-spliced bars with different grout resistance and the case diameter. They proposed the splice length equal to 16 times of the nominal diameter of bar, in order to have proper tensile strength. Also, in order to suppress bar slip in grout, slippage between bars and the case should be negligible. Sayadi *et al*. (2014) tested a kind of bolted splicing under pure bending; their results showed that this kind of splicing performed satisfactorily, in certain splicing length. Nguyen *et al*. (2013) studied on four types of mechanical patches. Three of them were only in different engagement length between the bars and coupler. The fourth one not only had more engagement length than the others but also its inner part was filled with epoxy. The results showed that the fourth one had better performance than the others. Hosseini *et al*. (2015) introduced a new kind of bar splice that was very similar to the injection splice but it used spiral wrap instead of steel case. Ling *et al*. (2012) studied two kinds of injection splices with cylindrical and conical cases. It was concluded that performance of the conical case provided better integrity than the cylindrical one. Moradi *et al*. (2012) studied on design parameters of injection-splicing such as; diameter and wall thickness of the case, material and length of the case, chemical and mechanical specification of grout as well as optimal designing of inner cross-section of the case. Mohammadzade *et al*. (2010) assessed the ductility of patched reinforced concrete beams, and concluded that concrete compression strength and also volume of stirrups have remarkable effect on the ductility of patched reinforced beams.

2. Research significance

Experimental research is required to verify replacement of overlapping by forging in splicing of the steel bars in RC parts, in different details and conditions. Tests on reinforced concrete members should be conducted in which steel bars -particularly in higher diameter- are patched together at different positions by forging method. These tests are specifically needed for some special high-rise buildings and long-span bridges to reduce the volume and cost of reinforcing. This point represents serious concerns and also the objective of this research on its beneficially for specific structures with high congestion in longitudinal reinforcement, in where enough spacing between bars is expected to be provided by eliminating lap splicing of the steel bars. Therefore, an experimental research has been conducted to investigate the behavior of concrete beams reinforced by the bars with forging splicing, and to obtain their capacity, ductility and energy dissipation to develop design and detailing requirements for these sort of members. Four concrete beam specimens with the same dimensions and reinforcing details but in different style of splicing (no splice, 100% overlap splicing, 50%, and 100% forging splicing) were designed, constructed, and tested under monotonic loading. The results of the tests are summarized in the following sections with the assessment of their significance from capacity and ductility performance perspective.

3. Experimental program

3.1 Specimens details

There were four beams with companion dimensions and reinforcement arrangement shown in Figs. 1 and 2. One of them as reference specimen had continuous bars with no connection, and

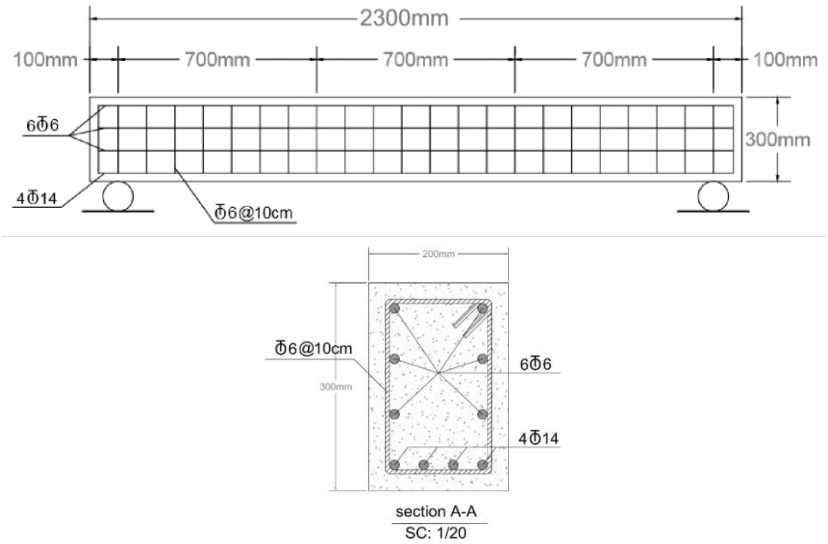

Fig. 1 The cross section and reinforcement arrangements of tested specimens

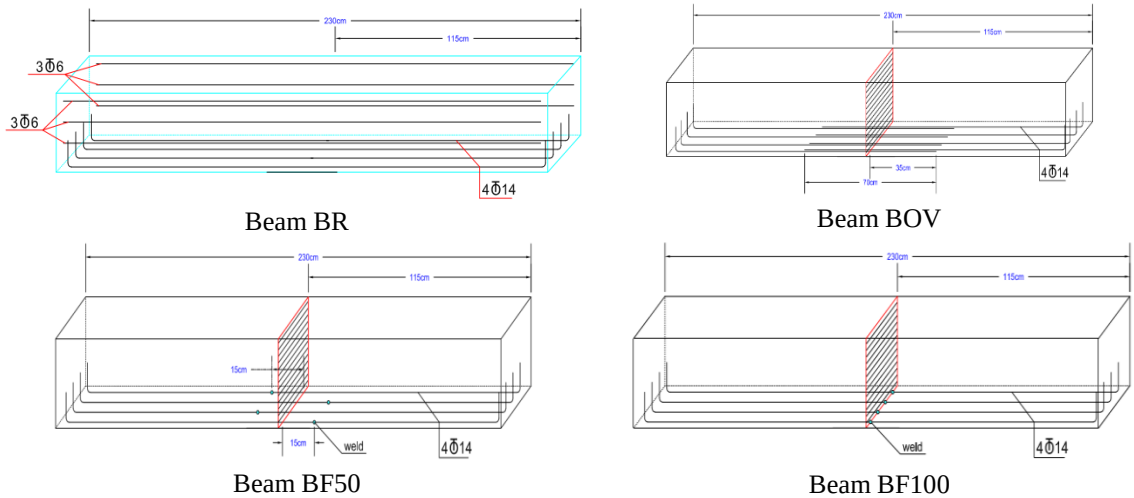

Fig. 2 Details of longitudinal rebars connection in tested beams

other three beams with different connections were tested under four-point loading system. The total length of beam was 2300 mm and clear distance between two hinged supports was 2100 mm, the distance between concentrated forces was equal to 700 mm. The width and height of beams' cross-section were selected 200 and 300 mm, respectively. Four rebars with diameter of 14 mm as main flexural tensile rebars were put in the lowest parts of beams with 6 mm rebar as stirrups. Furthermore, six 6 mm diameter rebars were used in three different rows to install strain gauges in the height of beam in order to calculate changes of strains. The names and details of four tested beams is shown in Table 1.

Strain gauges, Linear Variable Differential Transformer (LVDT), and load cell were used respectively to measure strains, displacements, and applied loads. Fig. 3 shows the experimental

Table 1 Details and specification of tested beams

No.	Specimen	Details
1	BR	**B**eam as **R**eference (without forging or overlap)
2	BOV	**B**eam with **Ov**er-lapping bars
3	BF50	**B**eam with **F**orging -**50**%
4	BF100	**B**eam with **F**orging-**100**%

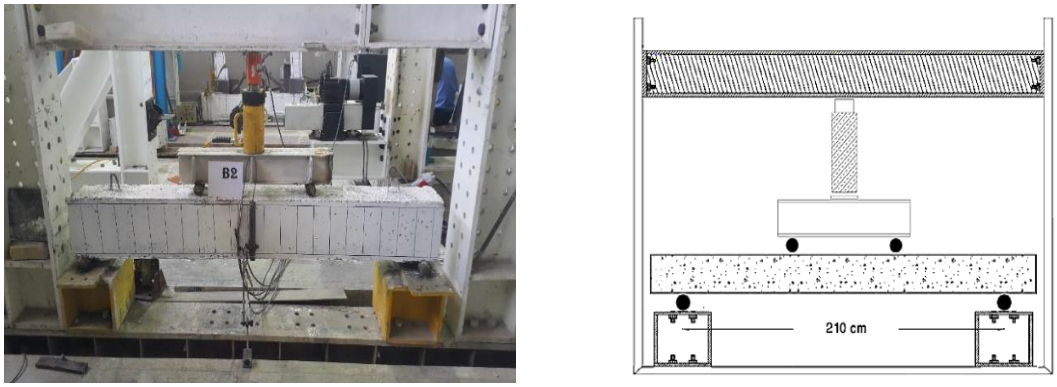

Fig. 3 Experimental and schematic set-up loading

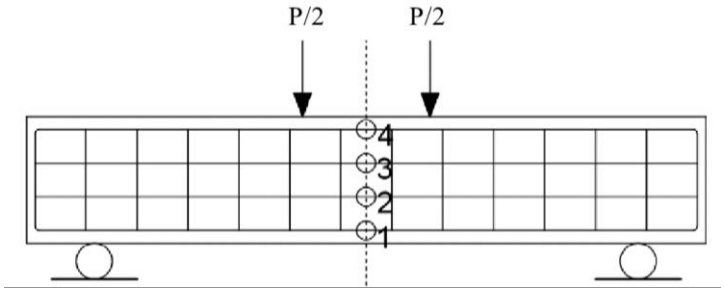

Fig. 4 Loading system and installation points of strain gauges

and schematic set-up loading. Four strain gauges were installed according to Fig. 4 at the height of each beam; in the bottom, middle, and top of beam. Load was increasingly exerted on the simple-supports beams in two-point state with distance of 700 mm.

3.2 Material properties and mix designs

In this research, gravel had 47% crushing, and its grains remained between sieves of 12.5 mm and 4.75 mm. Grading curve of the used sand and gravel are shown in Fig. 5. As it is shown, sand contained more coarse grains than the allowable limit. Type II Portland cement was used to make concrete. Concrete mix design for casting specimens is given in Table 2, with dry sand and gravel and water to cement ratio equal 0.4. The consumed water was more than calculated amount due to used dried aggregates. Six cubic samples of 15 cm were made in order to determine the compressive strength of concrete, resulting in 35 MPa in 28-day age, which is equivalent to 28 MPa for standard cylindrical sample.

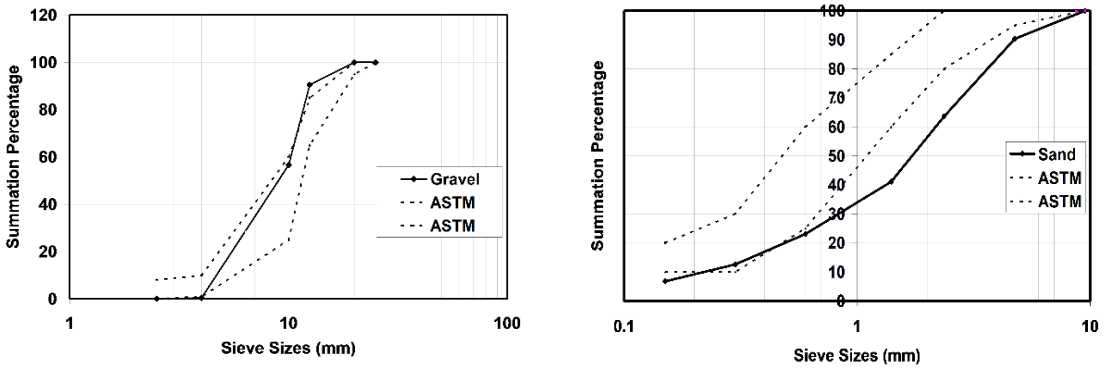

(a) Gravel (b) Sand

Fig. 5 Sand and gravel gradations curve

Table 2 Concrete mix design (1 m^3)

Final water	Primary water	Sand	Gravel	Cement	
--	0.4	1.55	2.85	1	Ratio
186	170	662	1222	429	Weight (kg)

4. Observations and primary results

The analysis of observations and obtained results of experimental works are main stage of a research to get essential information. Observations and primary results including load-displacement and load-strain curves, general behavior and crack pattern, ultimate strength, are presented in this section. Some other output results such as; ductility ratio, flexural stiffness, energy absorption, and so on to evaluate the effects of main parameters - i.e., patching style and percentage- on behavior of the samples are studied in the next section. Load- displacement curves of the samples are depicted in Fig. 6. The maximum capacity of the samples were 260, 262, 280, and 258 kN, for the BR, BOV, BF50 and BF100 sample beams, respectively. Cracking pattern of the specimens are shown in Fig. 7. Initial cracking of the BR, BOV, BF50 and BF100 samples were recorded at forces of 39, 47, 47 and 44 kN, respectively. Variation of the tensile and/or compressive strains are shown in Figs. 8 and 9, indicating that all tensile bars -in four beams- were reached to the yielding strain.

5. Results and discussion

According to the load-displacement curve, given in Fig. 6, yielding strength of the BR, BOV, BF50 and BF100 samples occurred at loads of 229, 249, 221 and 238 kN. Also, the maximum displacements of BR, BOV, BF50, BF100 samples at failure (degradation) point were 80.73, 88.53, 73.99 and 92.91 mm. All of these extracted results -from the load-displacement curves- are given in Table 3. The cracking, yielding, maximum (peak) and ultimate loads are denoted by P_{cr} (kN), P_y (kN), $P_{\max}$ (kN), and P_u (kN), with their corresponding displacements of Δ_{cr} (mm), Δ_y

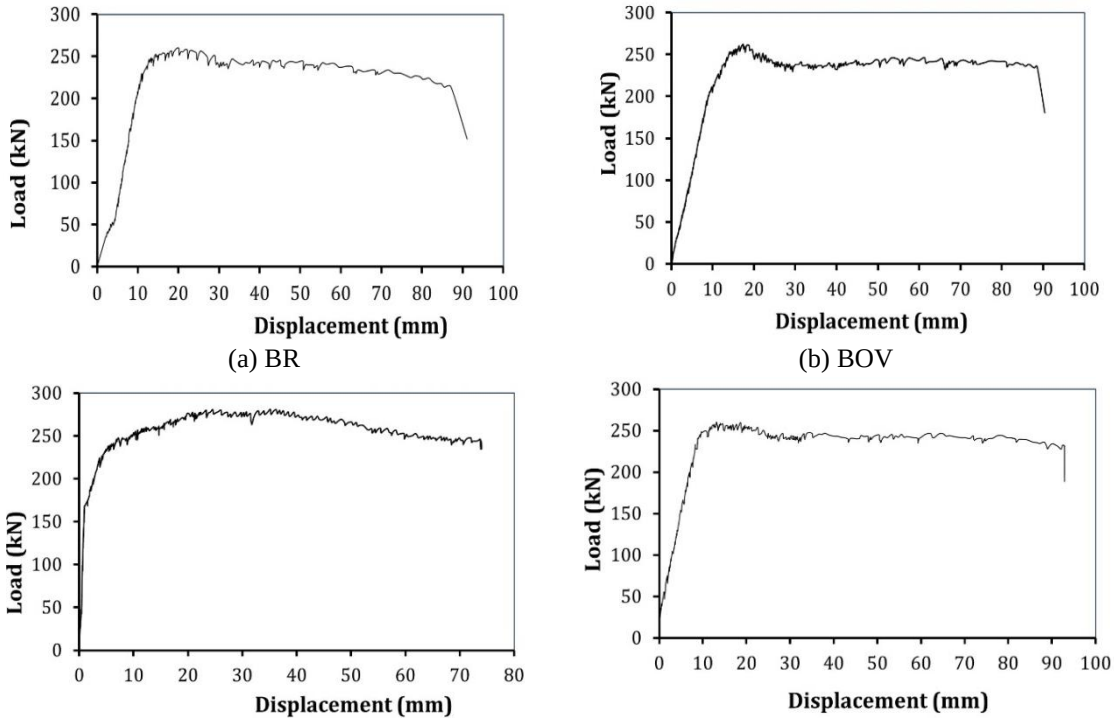

Fig. 6 Load-displacement curves in middle of beams

Table 3 Primary results of samples

Number	Name	P_{cr} (kN)	Δ_{cr} (mm)	P_{yr} (kN)	Δ_y (mm)	$P_{\max}$ (kN)	P_u (kN)	Δ_u (mm)
1	BR	39	3.12	229	11.41	260	221	8073
2	BOV	47	2.25	249	13.83	262	223	88.53
3	BF50	47	4.1	221	4.18	280	238	73.99
4	BF100	44	0.77	238	8.82	258	219	92.91

(mm), $\Delta_{\max}$ (mm); and Δ_u (mm), respectively. P_u defined as 0.85 $P_{\max}$ (kN) and its related displacement is Δ_u (mm), which are read from the curves in Fig. 6.

Ratio of all loads and displacements of three samples comparing to the reference specimen BR are shown in Table 4. According to Table 4, it is observed that yielding loads of samples were raised up to 8% in overlapped specimen (BOV), and 4% for the 100% forging specimen (BF100), whereas there was 4% reduction in load bearing capacity in the beam with 50% head to head welding (BF50). Therefore, the patching methods of the longitudinal bars had minor effect on the yielding strength of the RC beams. The yielding displacement was increased up to 20% in the overlapped specimen (BOV), whereas it significantly decreased up to 64% in the 50% forging beams (BF50). There was no significant changes (about 7%) in the maximum strengths due to patching methods of bars, but the ultimate displacements of the overlapped (BOV) and the 100% forging (Bf100) ones were increased up to 15% , while there was a decrease (up to 9%) in beam with 50% forging (BF50).

(a) BR

(b) BOV

(c) BF50

(d) BF100

Fig. 7 Crack pattern of tested beams

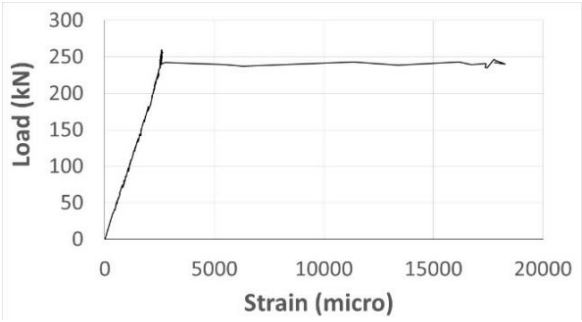

(a) BR

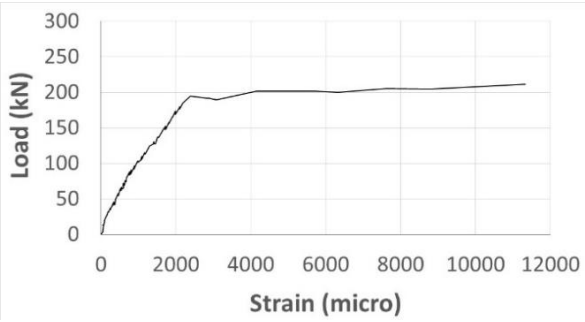

(b) BOV

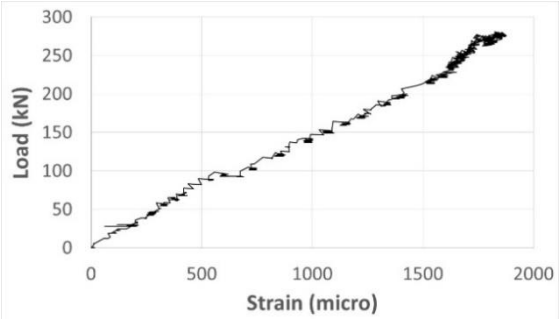

(c) BF50

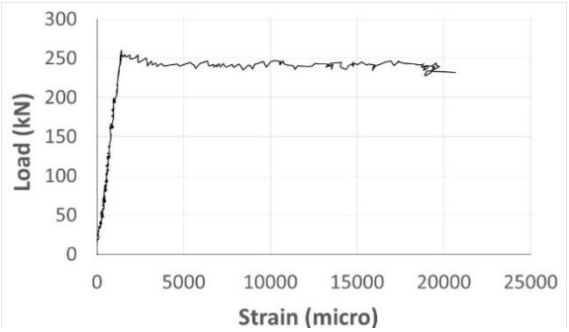

(d) BF100

Fig. 8 Load-strain variation curves of tensile rebar of beams

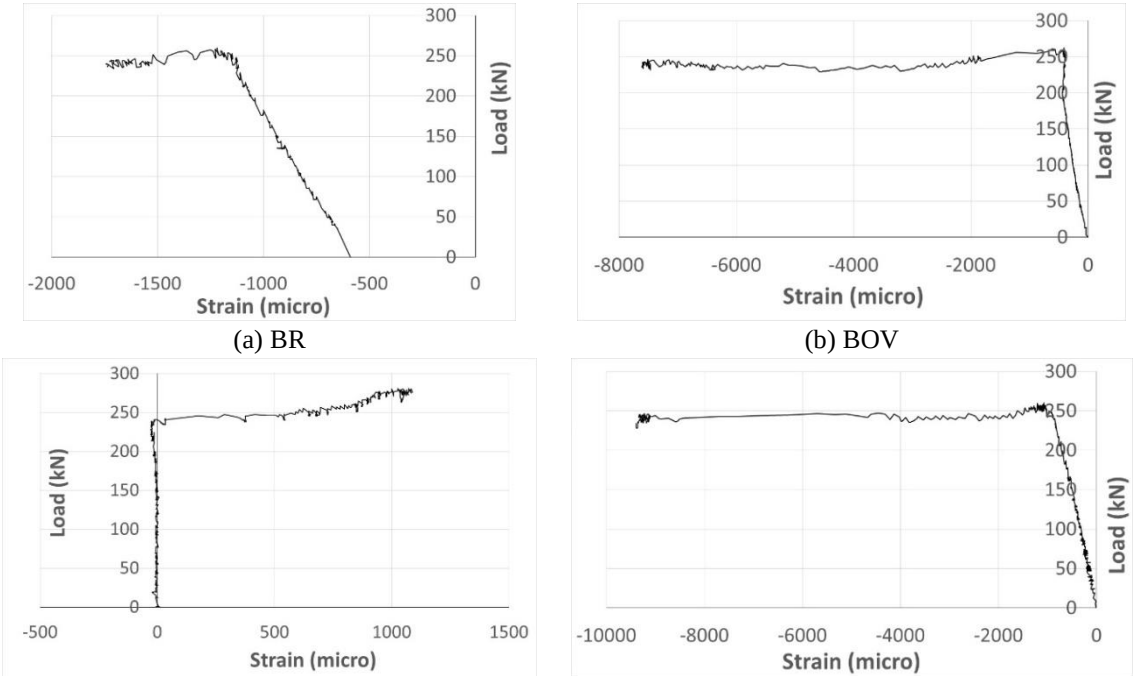

Fig. 9 Load-strain variation curves of compressive rebar of beams

Table 4 Comparison of results

Specimen	P_y (kN)	$\frac{P_{yi}}{P_{yBR}}$	Δ_y (mm)	$\frac{\Delta_{yi}}{\Delta_{yBR}}$	$P_{\max}$ (kN)	$\frac{P_{\max i}}{P_{\max BR}}$	Δ_u (mm)	$\frac{\Delta_{ui}}{\Delta_{uBR}}$
BR	229	1	11.41	1	260	1	80.73	1
BOV	249	1.08	13.83	1.21	262	1	88.53	1.09
BF50	221	0.96	4.18	0.36	280	1.07	73.99	0.91
BF100	238	1.04	8.82	0.77	258	0.99	92.91	1.15

Linear behavior is theoretically assumed for the strain variations in height of each concrete beam section. Four strain gauges were installed on the bars at the height of each specimen to measure real strain distribution via connecting strain amounts. The comparison of the assumed linear strain distribution and the actual non-linear experimental strain distributions of the four beams in five stages of yielding (at the yielding load, P_y), prior to yielding load (at the $0.75P_y$), maximum capacity (load $P_{\max}$), and twice of the yielding displacement ($2\Delta_y$), and ultimate displacement (Δ_u) are shown in Fig. 10. The charts showed that changing rate of the strains in all samples especially after yielding points was nonlinear.

5.1 Displacement and curvature ductility ($\mu_{\Delta i}$, $\mu_{\varphi i}$)

The Curvature at each loading case at each section of a flexural beam is equal to the ratio of the maximum compressive strain to its height from neutral axes. The real experimental compressive

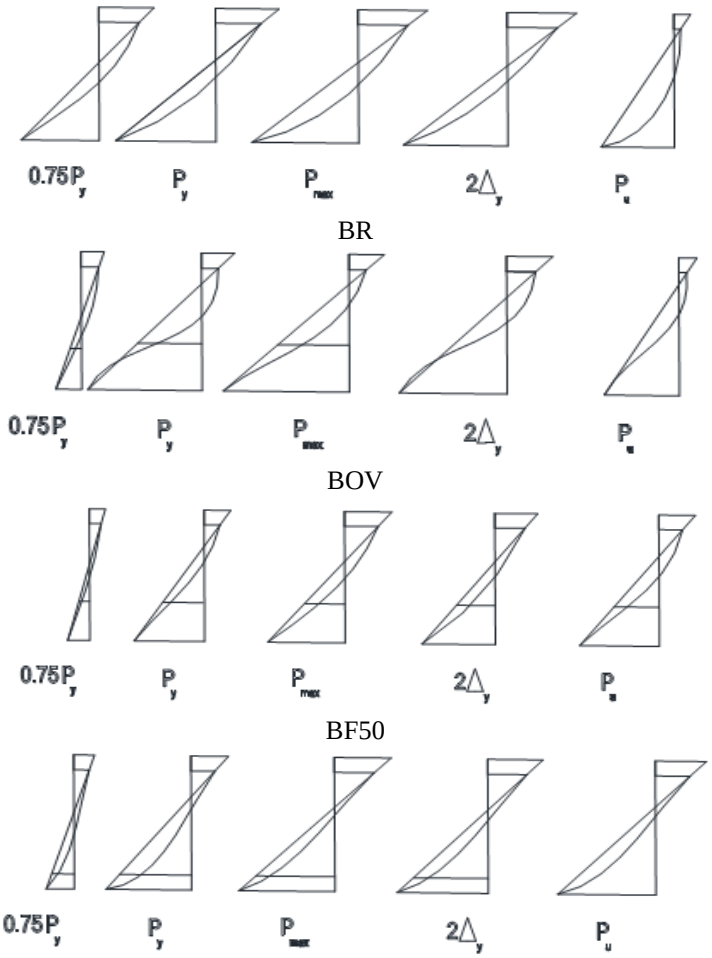

Fig. 10 Strain changes at the height of beams

Table 5 Results of curvature for beam samples

Specimen	ε_{cy}	x_y (mm)	$\varphi_y(\frac{1}{mm})$ (10^{-5})	ε_{cu}	x_u (mm)	$\varphi_u(\frac{1}{mm})$ (10^{-5})
BR	0.0014	119.3	1.17	0.0048	90.1	5.3
BOV	0.0012	110.5	1.28	0.0042	82.2	5.1
BF50	0.0006	113.5	0.52	0.0038	85.5	4.4
BF100	0.0009	112.6	0.79	0.0043	92.6	4.6

strain of concrete at each case of loading was calculated based on the strains in tensile and compressive rebars at mid-span of each sample, by assumption of linear strain distribution. Therefore, the calculation of the ultimate compressive strain based on strain variation at its height from the neutral axes for four samples are shown in Fig. 11. Also, the amounts of curvature in two cases of yielding and ultimate strengths of the specimens were calculated and depicted in Table 5.

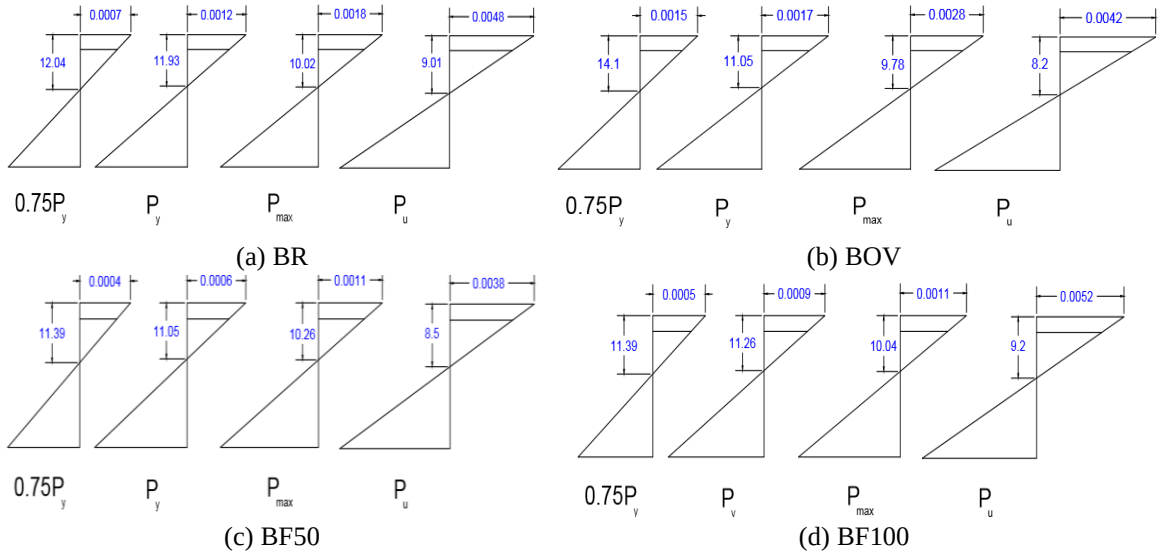

(a) BR (b) BOV

(c) BF50 (d) BF100

Fig. 11 Final compressive strain and height of neutral axes tested specimens

Displacement ductility ($\mu_{\Delta i}$) is defined as the ratio of ultimate displacement to the yielding one, and curvature ductility ($\mu_{\varphi i}$) is ratio of the ultimate curvature to the yielding one. Therefore, the displacement and curvature ductility values were calculated and given in Table 6, based on those values were given in Tables 4 and 5. The results show that the displacement ductility of forge welding beams were increased up to 2.5 times of the reference beam, while this ductility had 10% reduction for the overlapped one. The same trend is observed for the curvature ductility, as it were increased up to 86 percent in 50% forging beam while curvature ductility of overlap beam was decreased up to 12%.

Table 6 Results of displacement and curvature ductility of beams

Specimen	Δ_y (mm)	Δ_u (mm)	μ_Δ	$\frac{\mu_{\Delta i}}{\mu_{\Delta BR}}$	$\varphi_y\,(\frac{1}{mm})\ (10^{-5})$	$\varphi_u\,(\frac{1}{mm})\ (10^{-5})$	μ_φ	$\frac{\mu_{\varphi i}}{\mu_{\varphi BR}}$
BR	11.41	80.73	7.07	1	1.17	5.3	4.5	1
BOV	13.83	88.53	6.4	0.9	1.28	5.1	3.9	0.88
BF50	4.18	73.99	17.7	2.5	0.52	4.4	8.4	1.86
BF100	8.82	92.91	10.53	1.49	0.79	4.6	5.8	1.29

Table 7 Percentage of energy absorption of samples

Specimen	Energy absorption E (kN-mm	$\frac{E_i}{E_{BR}}$
BR	21403	1
BOV	21404	1
BF50	25485	1.19
BF100	23668	1.1

5.2 Energy absorption of samples

Energy absorption is equal to area under load -displacement curve. Therefore, the amounts of energy absorption of four specimens is given shown in Table 7. Table 7 shows that the energy absorption of BOV, BF50 and BF100 specimens were 1, 1.19 and 1.1 times of that of reference beam. The comparison of results given in Tables 6 and 7 indicated that the effectiveness of forging connection particularly in specimen BF50 with 50% forging (about 80%) was in increasing ductility more than its effectiveness on energy absorption (about 20%).

5.3 Moment-curvature curve and effective flexural stiffness

The moment and curvature at each load were calculated and then moment-curvature curves of

Table 8 Comparison of effective flexural stiffness of beams

Specimen	$M_{\max}(kN-m)$	Equivalence $\varphi_y^{'}$ $(\frac{1}{mm})x10^{-7}$	E_cI_e (10^{13}) $(\mathrm{N-mm^2})$	E_cI_g (10^{13}) $(\mathrm{N-mm^2})$	$\alpha=\frac{E_cI_e}{E_cI_g}$	$\frac{\alpha_i}{\alpha_{BR}}$
BR	91	190	0.48	1.18	0.41	1
BOV	91.5	125	0.73	1.18	0.62	1.5
BF100	90	115	0.78	1.18	0.66	1.61

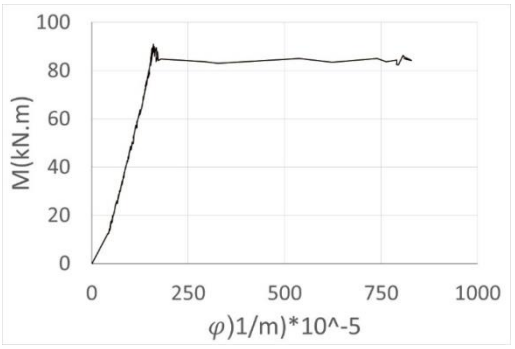

(a) BR

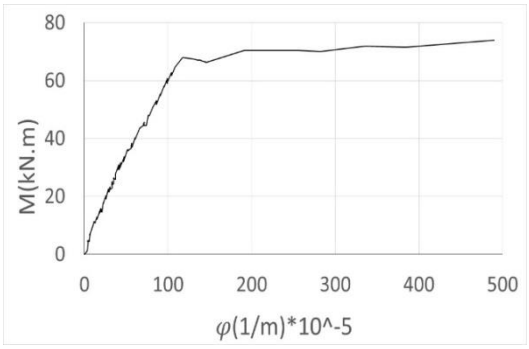

(b) BOV

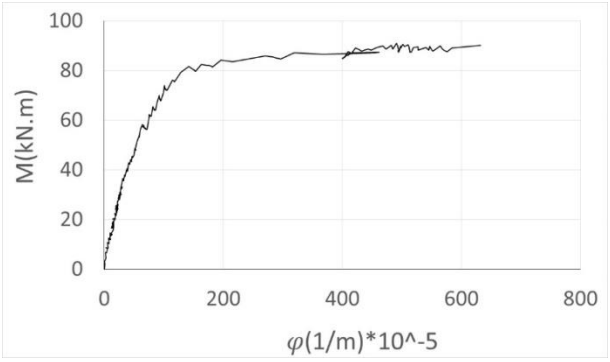

(c) BF100

Fig. 12 Moment- curvature curve of tested beams

four specimens are shown in Fig. 12. Amount of effective flexural stiffness ($E_cI_{e,eff}$) of each specimen is the slope of idealized two-line curve on the real moment-curvature chart M-ϕ, therefore the ratio of maximum moment to equivalence curvature ($\frac{M_{\max}}{\phi_y'}$) is the effective flexural stiffness of sample. These amounts can be compared with total uncracked flexural stiffness ($E_cI_{g,}$). Modulus of elasticity for concrete and inertia moment of the entire sample is gotten by relations $E_c = 5000\sqrt{f_c'}$ and $I_g = \frac{bh^3}{12}$, respectively. Ratio of effective flexural stiffness to total flexural stiffness is defined as $\alpha = \frac{E_cI_e}{E_cI_g}$. This ratio is calculated in Table 8 and showed that the ratio of BR, BOV, and BF100 samples were 0.41, 0.62, and 0.66. And also the results showed that the effective stiffness of BOV (with overlapping rebars) and BF100 (100% forging) samples were about 60% more than effective stiffness of beam sample with universal rebars without splice.

5.4 General effect of lap and welded splice in comparison to rebars without splice

The load-displacement curves of reference BR specimen with continuous rebars were compared with those of BOV specimen with 100% bars overlapping) in Fig. 13 in order to assess the effect of overlapping. As observed from Fig. 13 and comparison given in Table 9, both specimens had almost same general behavior with same maximum capacity and energy absorption, but most of fractures in beam with overlapping rebar were happened in two support bearings as shown in Fig. 7. Furthermore, it was observed that splicing of longitudinal rebar caused the yield load and displacement to be increased by 8, 21% with same maximum capacity. When comparing between ductility of two beams, it was known that splicing of longitudinal rebar caused displacement and curvature ductility of beam to be decreased by 10 and 15%, otherwise the effective flexural stiffness of overlapped beam was increased up to 50%.

Table 9 Comparison of "reference beam" with "beam with overlapping rebar"

$\frac{\alpha_i}{\alpha_{BR}}$	$\frac{E_i}{E_{BR}}$	$\frac{\mu_{\varphi i}}{\mu_{\varphi BR}}$	$\frac{\mu_{\Delta i}}{\mu_{\Delta BR}}$	$\frac{\Delta_{yi}}{\Delta_{yBR}}$	$\frac{\Delta_{ui}}{\Delta_{uBR}}$	$\frac{P_{\max i}}{P_{\max BR}}$	$\frac{P_{yi}}{P_{yBR}}$	Specimen
1.5	1	0.85	0.9	1.21	1.09	1	1.08	BOV

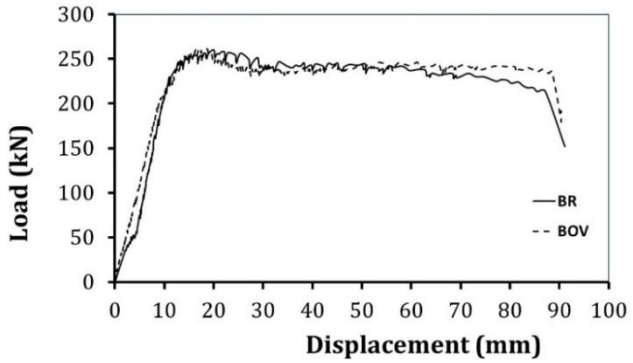

Fig. 13 Load-displacement curve of BR and BOV beams

The another comparison was done between BR specimen with no connection bar and BF50 and BF100 specimens with 50 and 100% head to head welding in Fig. 14 and Table 10 in order to assess the effect of 50 and 100% forging. As shown in Fig. 7, the forging beams experienced more cracks with less severe damage prior to failure comparing to reference beam with continuous bars. The forging had the positive effect up to 7% on maximum capacity and significant increasing on both displacement and curvature ductility up to 150 and 86%, respectively. Although the total energy absorption was increased up to 10%, but more increasing up to 61% in effective stiffness was observed.

The comparison of BF50 and BF100 specimens with 50 and 100% forging results was done in Fig. 15 and Table 11. In Fig. 7, the crack pattern behaviors of two samples were same but the most damages in BF100 beam were happened in the middle of beam due to concentrated stress of 100% forging in that point comparing with 50% forging at two different points. The specimen with 50% forging in each section had higher maximum capacity up 10 8% and valuable increasing in both ductility up to 70%, therefore both maximum strength and ductility performance of beam with 50% forging were better than companion beam with 100% forging.

In order to compare the welding and overlap connections effects, load–displacement curves with related results shown and given in Fig. 16 and Table 12. Forging beams had more damages at the failure cases comparing to overlapping beam according to Fig. 7. BF100 beam with 100% forging had the same general behavior, energy absorption and capacities with BOV overlapping beam, but 100% forging beam showed more than 50% increasing in ductility and effective stiffness. The 50% forging beam had better behavior with higher effectiveness, 7% increasing in

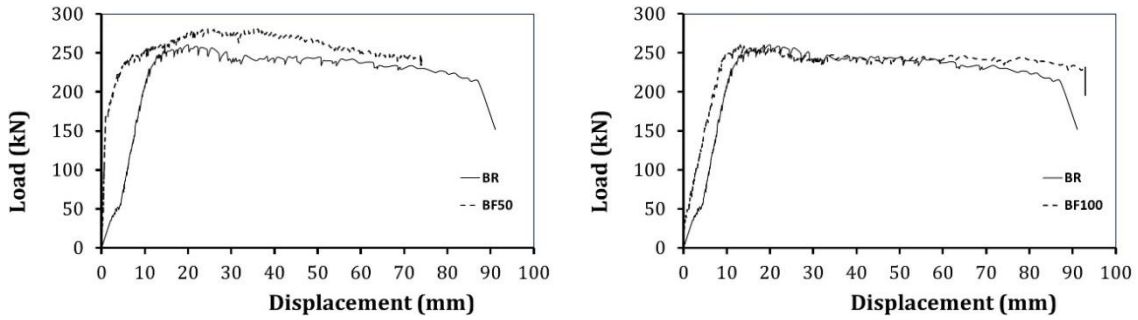

Fig. 14 Comparison of load-displacement curves of BR with BF50 and BF100 beams

Table 10 Comparing reference beam and beams with rebar of forging welding

$\frac{\alpha_i}{\alpha_{BR}}$	$\frac{E_i}{E_{BR}}$	$\frac{\mu_{\varphi i}}{\mu_{\varphi BR}}$	$\frac{\mu_{\Delta i}}{\mu_{\Delta BR}}$	$\frac{\Delta_{yi}}{\Delta_{yBR}}$	$\frac{\Delta_{ui}}{\Delta_{uBR}}$	$\frac{P_{\max i}}{P_{\max BR}}$	$\frac{P_{yi}}{P_{yBR}}$	Specimen
-	0.73	1.86	2.5	0.36	0.91	1.07	0.96	BF50
1.61	1.1	1.29	1.49	0.77	1.15	0.99	1.04	BF100

Table 11 Comparing of beams with forging rebar of 50 and 100%

$\frac{E_i}{E_{BF100}}$	$\frac{\mu_{\varphi i}}{\mu_{\varphi BF100}}$	$\frac{\mu_{\Delta i}}{\mu_{\Delta BF100}}$	$\frac{\Delta_{yi}}{\Delta_{yBF100}}$	$\frac{\Delta_{ui}}{\Delta_{uBF100}}$	$\frac{P_{\max i}}{P_{\max BF100}}$	$\frac{P_{yi}}{P_{yBF100}}$	Specimen
0.66	1.5	1.7	0.47	0.79	1.08	0.92	BF50

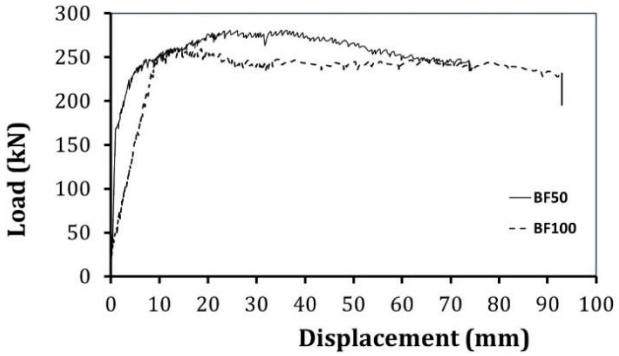

Fig. 15 Comparison of load-displacement curves of BF50 with BF100 beams.

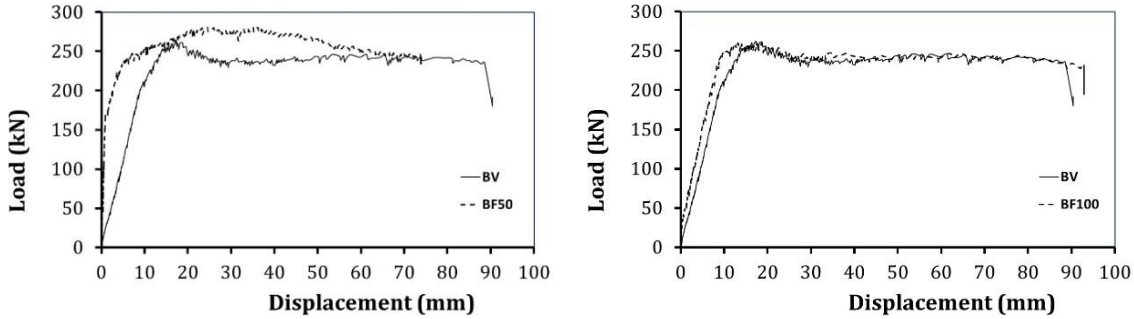

Fig. 16 Curve of load-replacement of BOV beam with BF50 and BF100 beam

Table 12 Comparing overlapping beam and beams with rebar of forging welding

$\frac{\alpha_i}{\alpha_{BOV}}$	$\frac{E_i}{E_{BOV}}$	$\frac{\mu_{\varphi i}}{\mu_{\varphi BOV}}$	$\frac{\mu_{\Delta i}}{\mu_{\Delta BOV}}$	$\frac{\Delta_{yi}}{\Delta_{yBOV}}$	$\frac{\Delta_{ui}}{\Delta_{uBOV}}$	$\frac{P_{\max i}}{P_{\max BOV}}$	$\frac{P_{yi}}{P_{yBOV}}$	Specimen
-	0.73	2.19	2.78	0.30	0.84	1.07	0.88	BF50
1.61	1.1	1.52	1.66	0.64	1.06	0.99	0.96	BF100

capacity and more than 120 and 180% increasing in displacement and curvature ductility.

The general results of specimens showed that even though the forging method inducing to probable brittle bar comparing to other splicing method or bars without splice, but the global performance of specimens including ductility and energy dissipation were increased, therefore there is no negative effect of application of forging method for bar splicing.

6. Conclusions

Four reinforced concrete beams with companion cross section, bar arrangement and material but with four different bar connections of continuous, overlapping, and 50% and 100% forging were cast and experimentally tested under four-point loading system. Based on observations and obtained discussions, the following results are obtained:

• The connection method for longitudinal rebar of flexural Reinforced Concrete beams had

different effects on the yield and maximum and ultimate strength and displacements and also on energy absorption and ductility and effective stiffness indexes.

• The overlapping system had same ultimate strength with continuous system but with up to 10 and 50% increasing in yielding strength and effective stiffness with up to 15% decreasing in both displacement and curvature ductility.

• The both beams with 50 and 100% forging of longitudinal rebar showed the better behavior and results than beam with continuous bars.

• 50% forging beam had 7, 150, and 86% increasing in strength, displacement and curvature ductility comparing to continuous bar beam, while its yielding strength, displacement and energy absorption were decreased.

• 100% forging beam had same ultimate strength with continuous bar beam, but its displacement and curvature ductility, energy absorption, and effective stiffness were increased up to 49, 29, 10, and 61%.

• Overall the 50% forging beam had better behavior than 100% forging beam with up to 10 and 70% increasing in strength and ductility.

• The comparison of forging and overlapping bar beams indicated that the forging bar beams had minor increasing in strength but significant increasing in flexural ductility for particular purpose applications.

References

ACI 318-2014 (2014), American Concrete Institute.

Bagheri, K. and Fasihi, H. (2013), "Optimization of RC building", *Iran Annual Concrete Conference.* (in Persian)

Camille, A. and Nasr, I. (2006), "An experimental study of welded splices of reinforcing bars", *Build. Environ.*, **41**(10), 1394-1405.

Coogler, K. (2006), "Investigation of the behavior of offset mechanical splices", Doctoral Dissertation, University of Pittsburgh.

EL-Hacha, R., Elagroudy, H. and Rizkalla, S. (2004), "Proposed modification to the ACI 318-02 Code equation on bond strength for steel bars", *5th Structure Specialty Conference of the Canadian Society for Engineering*, Saskatoon, Saskatchewan, Canada.

Henin, E. and Morcous, G. (2014), "Non-proprietary bar splice sleeve for precast concrete construction", *Eng. Struct.*, **83**, 154-162.

Hosseini, J., Baharuddin, A., Mohd Hanim, R. and Saim, A. (2015), "Bond behavior of spirally confined splice of deformed bars in grout", *Constr. Build. Mater.*, **80**, 180-194.

Hua, L., Baharuddin, A. and Rahman, I. (2014), "Feasibility study of grouted splice connector under tensile load", *Constr. Build. Mater.*, **50**, 530-539.

Iran Building National Regulations (2013), 9-Code, Design and Construction RC Building, 4th Version, Road and Urbanization Ministry. (in Persian)

Ling, J., Baharuddin, A., Izni syahrizal Abrahim, R. and Abdul hamid, Z. (2012), "Behavior of grouted pipe splice under incremental tensile load", *Constr. Build. Mater.*, **33**, 90-98.

Mccabe, S. (2000), "The performance of mechanical splices", *12WCEE, 12th World Conference on Earthquake Engineering*.

Mohamadzade, B., Esfahani, M.R. and Shoushtari, A. (2010), "Investigation of ductility of spliced RC beams", *Ferdousi Civil Eng. J.*, **22**(1). (in Persian).

Moradi Shashaghi, T., Faramazzade, V. and Jahfarnezhad, H. (2012), "Evaluation of performance of mechanical splices of tensile bars, steel filled concrete tubes in RC members", *Iran Annual Concrete*

Conference. (in Persian)
Navaratnarajah, V. (1983), "Splicing of reinforcement bars with epoxy joints", *NT. J. Adhes. Adhes.*, **3**(2), 93-99.
Nguyen, D., Mutsuyoshi, R. and Ohno, T. (), "Experimental study on RC beams using mechanical splices with different quality and staggering length", *Proceedings of the Thirteenth East Asia-Pacific Conference on Structural Engineering and Construction (EASEC-13).*
Park, S., Choib, S., Stubbs, N., Bolton, R., Price, A. and Sikorsky, C. (2008), "A modal parameter based technique to inspect welded reinforcement splices", *Eng. Struct.*, **28**(3), 453-465.
Reetz, R., Ramin, V. and Matamoros, A. (2013), "Performance of reinforcement coupler systems", *Pacific Conference Earthquake Engineering*.
Sayadi, A., Baharruddin, A., Bin Jumaat, M.Z. and Johnson, R.U. (2014), "The relationship between interlocking mechanism and bond strength in elastic and inelastic segment of splice sleeve", *Constr. Build. Mater.*, **55**, 227-237.
Tahouni, Sh. (1996), *Design of RC Building*, Tehran University Press. (in Persian)
Turk, K. and Yildirim, M.S. (2003), "Bond strength of reinforcement in splices in beams", *Struct. Eng. Mech*, **16**(4), 469-478.
UBC97 (1997), Design Code.

JK